

Dynamics of Rigid and Flexible Extended Bodies in Viscous Films and Membranes

Alex J. Levine,^{1,2} T. B. Liverpool,^{1,3} and F. C. MacKintosh^{1,4}

¹The Kavli Institute for Theoretical Physics, University of California, Santa Barbara, California 93106, USA

²Department of Physics, University of Massachusetts, Amherst, Amherst, Massachusetts 01060, USA

³Department of Applied Mathematics, University of Leeds, Leeds LS2 9JT, United Kingdom

⁴Division of Physics & Astronomy, Vrije Universiteit, 1081 HV Amsterdam, The Netherlands

(Received 6 June 2003; published 15 July 2004)

We study the dynamics of extended rodlike bodies in (or associated with) membranes and films. We demonstrate a striking difference between the mobilities in films and bulk fluids, even when the dissipation is dominated by the fluid stress: For large inclusions, we find that rotation and motion perpendicular to the rod axis exhibit purely local drag, in which the drag coefficient is algebraic in the rod dimensions. We also study the dynamics of the *internal* modes of a semiflexible inclusion and find two dynamical regimes in the relaxation spectrum.

DOI: 10.1103/PhysRevLett.93.038102

PACS numbers: 87.68.+z, 83.10.-y, 87.16.Dg

The mobility of inclusions in membranes is a fundamental physical parameter controlling a number of cellular processes. Since inclusions such as proteins [1,2] or “rafts” [3,4] can in many cases be large compared to the constituent lipids of the membrane, they can be viewed as macroscopic objects moving in a continuum fluid environment. The dynamics of these objects in thin films has already been shown to be surprisingly subtle, leading to confusion in the early literature on protein diffusion in cell membranes [5]. This was largely clarified by Saffman and Delbrück [6], who noted that motion of objects in or attached to a (2D) membrane is never strictly two dimensional since in-plane momentum induces flows in the surrounding bulk (3D) fluid. This viscous coupling of the interface to the surrounding fluid introduces a new length scale $\ell_0 \sim \eta_m/\eta_f$ determined by the ratio of the (2D) membrane viscosity η_m and the (3D) fluid viscosity η_f . This length determines the degree to which the dissipation is predominantly two or three dimensional [5–12]. As a result, the drag coefficient on a small object in a membrane is a nonlinear function of both its size and the membrane viscosity. For example, the diffusion coefficients of small proteins (linear size $< \ell_0$) in membranes have a weak (logarithmic) dependence on their size.

Here, we examine the motion of rodlike inclusions in viscous films and membranes, as a representative example of a general problem of mobility of arbitrary extended bodies. The generalization of this problem to motion in viscoelastic films is straightforward [10–12]. Our work is motivated in part by the prospect of computing mobilities of proteins and lipid rafts in lipid bilayers [1–4], as well as by recent experiments that have demonstrated the possibility of making quantitative rheological measurements of viscoelastic films resembling cellular structures such as the *actin cortex* [10] using tracer particle fluctuations (membrane microrheology). The driven motion of rods in viscous/viscoelastic films has also been used to determine rheological properties, e.g., of monolayers

[13,14], for which the approach we develop here is important. We also analyze the undulatory motion of semiflexible polymers at a membrane surface, and find two dynamical regimes, one of which exhibits purely local hydrodynamic drag in contrast to 3D liquids.

Our calculation of the hydrodynamic drag ζ on a *rigid* rod of length L and radius a gives two principal results: (i) For small objects (specifically, $L \ll \ell_0$), the drag coefficients become independent of both the rod orientation and aspect ratio; and (ii) for larger rods of high aspect ratio, ζ_{\perp} becomes purely linear in the rod length L —i.e., the drag becomes purely local. In contrast, we find that the well-established three-dimensional result $\zeta_{\parallel} = 2\pi\eta_f L / \ln(AL/a)$ (where A is a number of order unity) applies for parallel motion in the film, provided that $L \gg \ell_0$. Here, however, the effective rod radius becomes ℓ_0 rather than the physical radius a , when $a \ll \ell_0$. Closely related to (ii), we find that the rotational drag (equivalently diffusion constant) depends purely algebraically on the rod length. For motion perpendicular to the rod (and rotation), the qualitative difference between 3D hydrodynamic drag on a rod and membrane-bound motion arises from the incompressibility of the interfacial material which dramatically changes the flow field in-plane and in the surrounding fluid.

We begin with the response of the two-dimensional membrane to an in-plane force. This is calculated by solving the coupled equations for in-plane and out-of-plane fluid motions, taking into account incompressibility [11] of both the bulk and the membrane. The in-plane velocity $v_{\alpha}(\mathbf{x})$ at position \mathbf{x} resulting from a point force $f_{\beta}(\mathbf{x}')$ at *another* point \mathbf{x}' is $v_{\alpha}(\mathbf{x}) = \chi_{\alpha\beta}(\mathbf{x} - \mathbf{x}')f_{\beta}(\mathbf{x}')$. The response function $\chi_{\alpha\beta}(\mathbf{x})$ is

$$\chi_{\alpha\beta}(\mathbf{x}) = \chi_{\parallel}(|\mathbf{x}|)\hat{x}_{\alpha}\hat{x}_{\beta} + \chi_{\perp}(|\mathbf{x}|)[\delta_{\alpha\beta} - \hat{x}_{\alpha}\hat{x}_{\beta}], \quad (1)$$

where the scalar functions χ_{\parallel} , χ_{\perp} of the distance between the point of the force application and the measurement of the velocity field are given by [15]

$$4\eta_m\chi_{\parallel}(x) = \frac{\mathbf{H}_1(z)}{z} - \frac{2}{\pi z^2} - \frac{Y_0(z) + Y_2(z)}{2}, \quad (2)$$

$$4\eta_m\chi_{\perp}(x) = \mathbf{H}_0(z) - \frac{\mathbf{H}_1(z)}{z} + \frac{2}{\pi z^2} - \frac{Y_0(z) - Y_2(z)}{2}, \quad (3)$$

where the \mathbf{H}_ν are Struve functions, and the Y_ν are Bessel functions of the second kind. Here, $z = |\mathbf{x}|/\ell_0$ is the distance between the point of force application and the membrane velocity response in units of ℓ_0 . This length is given by $\ell_0 = \eta_m/\eta_f$ for a Langmuir monolayer, where the subphase fluid viscosity is η_f . For a membrane with fluid on both sides, $\ell_0 = \eta_m/(2\eta_f)$.

There are three independent drag coefficients and corresponding mobilities. In-plane rotational and inversion symmetries of the rod imply that the mobility tensor has the form $\mu_{ij} = \mu_{\parallel}\hat{n}_i\hat{n}_j + \mu_{\perp}(\delta_{ij} - \hat{n}_i\hat{n}_j)$. Here μ_{\perp} and μ_{\parallel} are the mobility of the rod dragged perpendicular to and parallel to its long axis (the \hat{n} direction), respectively. In addition to these, there is also one rotational mobility, μ_{rot} , linking the angular velocity of the rod to the torque applied to that rod about its center of inversion symmetry.

We solve the problem by two complementary methods that are useful for the regimes of small and large aspect ratios, respectively. For nearly circular objects, $1 < L/a \leq \mathcal{O}(10)$, we use a 2D analogue of the Kirkwood approximation [16] to model the continuous rod by a series of disks subject to point forces at their centers. This method becomes rather cumbersome for rods much longer than their cross-sectional radius, i.e., $L \gg a$, but here we use a second approximation for infinitely thin rods. In both cases, we restrict our attention to the limit $a \ll \ell_0$. Below, we illustrate both methods by a calculation of the transverse drag coefficient with the understanding that the longitudinal and rotational drag proceed analogously.

The linearity of the underlying low-Reynolds number hydrodynamics allows us to use superposition. Specifically, we replace the rod of length L and cross-sectional radius a by a set of $N + 1$ thin disks of radius a lying in the membrane and having a center-to-center separation b chosen so that the total length of the rod is preserved; i.e., $L = Nb + 2a$. We maximize the number of disks consistent with the given aspect ratio of the rod and the non-interpenetrability of the disks.

Our strategy for computing the drag on the rod involves setting the rod in uniform motion with unit velocity by imposing some set of forces $\mathbf{f}^{(i)}$, $i = 1, \dots, N + 1$ on the $N + 1$ disks making up the rod. We can use the response function to compute the velocity field for a given collection of point forces $\mathbf{v}_{\parallel,\perp}^{(i)} = \sum_{j=1}^{N+1} \chi_{\parallel,\perp}^{(ij)} f_{\parallel,\perp}^{(j)}$. However, we must demand that all the disks have the *same* velocity and thereby determine the forces applied to them. To enforce this constraint, we invert the matrix $\chi_{\parallel,\perp}^{(ij)}$. The drag coefficient is then $\zeta_{\perp,\parallel} = \sum_{i,j=1}^{N+1} (\chi_{\perp,\parallel}^{-1})^{(i,j)}$.

For large N , i.e., high aspect ratio rods, the matrix inversion becomes difficult. To study that limit, one can assume an infinitely thin rod. Then, the velocity field at the point \mathbf{x} due to a continuous distribution of force densities along the rod, $\mathbf{f}(x\hat{x})$ that lie along the \hat{x} axis from $x = -L/2$ to $x = L/2$ takes the form

$$\mathbf{v}_{\alpha}(\mathbf{x}) = \int_{-L/2}^{L/2} \chi_{\alpha\beta}(\mathbf{x} - p\hat{x}) f_{\beta}(p\hat{x}) dp. \quad (4)$$

As before, we impose a unit velocity field on the rod and determine the required force, $\mathbf{f}(\mathbf{x})$. The inversion of Eq. (4) proceeds by first expanding the linear force density in Legendre polynomials $P_n(x)$ writing

$$f(x) = \sum_{n=0}^N c_{2n} P_{2n}(2x/L), \quad (5)$$

where the coefficients are as yet unknown. Since the Legendre polynomials form a complete set on the interval -1 to $+1$, any physical force density can be expressed as in Eq. (5) provided N be taken to infinity. In practice, we find excellent numerical results even when truncating this sum to just the first five terms.

We now impose the unit velocity condition at a finite set of points $0 \leq p_i \leq L/2$ along the rod since, if we truncate the Legendre function expansion of the force density at N , we can impose the velocity condition at a maximum of N points without creating an overdetermined system of equations. Thus, we require that $\mathbf{v}(p_i\hat{x}) = 1$, for $i = 1, \dots, N$. Now finding the force distribution along the rod requires only the inversion of an $N \times N$ matrix, \mathcal{N}_{ij} , whose components are defined by

$$\mathcal{N}_{ij} = \int_{-L/2}^{L/2} \chi(\hat{x}p_i - z\hat{x}) P_j(2z/L) dz. \quad (6)$$

Finally, the total force on the rod is found by reconstructing the force density from its Legendre polynomial expansion and integrating the resulting expression over the entire rod. That force density is given by Eq. (5) where the coefficients c_k are determined using the rod's unit velocity condition enforced at a discrete set of points along with the inverse of the matrix defined in Eq. (6). Thus, we find $c_k = \sum_{i=1}^N \mathcal{N}_{ki}^{-1}$. Because of the orthogonality of the Legendre polynomials, the total force is given entirely by the coefficient of the zeroth Legendre polynomial, and the total torque in the case of rotations is given by the coefficient of the first odd Legendre polynomial, c_1 . Numerically, we find a variation of less than a percent in the drag coefficient in all cases, so long as $N > 2$. Here, we report our results for $N = 5$. To check for consistency, we compared our results from this method and the Kirkwood approximation; for thin rods, we find excellent agreement.

The analogous calculation can be made for the drag on the rod moving in a direction perpendicular to its long axis [12]. We plot the parallel and perpendicular drag

coefficients for thin rods as a function of their length L/ℓ_0 in reduced units in Fig. 1. The convergence of the two drag coefficients when all dimensions of the rod are small compared to ℓ_0 reflects the weak dependence on shape and size of the Saffman-Delbrück result. For rods longer than this crossover length, these two drag coefficients diverge from each other, in marked contrast with the case of motion in bulk fluids, where the two drag coefficients differ by a constant multiple of 2.

For long rods ($L \gg \ell_0$), the parallel drag in the film is essentially unchanged from the bulk, three-dimensional drag, in that $\zeta_{\parallel} = (2\pi\eta_f L)/[\ln(0.43L/\ell_0)]$, where the prefactor in the logarithm has been determined to within 1%. Comparing with the result for drag of a rod in a bulk fluid, we see that the effective radius of the rod is now of order ℓ_0 (for $a \ll \ell_0$). Given that ℓ_0 corresponds to a length scale over which interfacial momentum densities flow into the bulk fluid due to the viscous coupling between the two, the system does not effectively resolve length scales smaller than ℓ_0 so the small dimension of the rod is replaced by this length. At large length scales (compared to ℓ_0), the fluid velocity field around the rod in parallel drag is the same as for rod motion in the bulk fluid; i.e., in both cases there should have been no flow from the plane of the interface into the surrounding fluid.

The case of perpendicular motion of long rods is qualitatively very different. Here we find $\zeta_{\perp} = 2\pi\eta_f L$ (see Fig. 1). For this case, the fluid flow field for a rod in bulk is inconsistent with the flow restrictions imposed by the presence of the interface. In 3D, there would be a nonvanishing two-dimensional divergence of velocity field restricted to the plane of motion of the rod. Now, the in-plane incompressibility of the interface requires that the fluid velocity field extend over distances comparable to the rod's largest dimension L . The standard

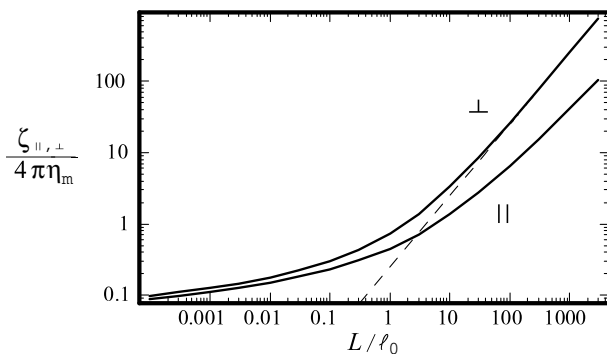


FIG. 1. Parallel (||) and perpendicular (⊥) drag coefficients for thin rods (i.e., high aspect ratio) of various lengths. For short rods both the parallel and perpendicular drag coefficients converge in a manner consistent with the Saffman-Delbrück result (not shown). The divergence between these two drag coefficients at long lengths reflects the absence of the hydrodynamic cooperativity (i.e., long-range hydrodynamic interactions) in the perpendicular case. The dashed line demonstrates that the perpendicular drag coefficient converges to $\zeta_{\perp} = 2\pi\eta_f L$ for rods longer than ℓ_0 .

038102-3

hydrodynamic coupling of portions of the rod, which gives rise to the logarithm in the drag is not present, resulting in a drag coefficient that is purely linear in rod length. In other words, the drag is effectively *local* or *free draining* in character. In three dimensions, in contrast, there is a length-independent ratio of 2 between the parallel and perpendicular drag coefficients because neither is free draining: $\zeta_{\parallel}^{3D} = (2\pi\eta_f L)/[\ln(\frac{AL}{a})]$ and $\zeta_{\perp}^{3D} = 2\zeta_{\parallel}^{3D}$.

The calculation of the rotational drag coefficient proceeds analogously to those of the perpendicular and parallel drag coefficients [12]. We plot the rotational drag coefficient divided by L^2 for a rod of infinite aspect ratio as a function of the reduced length in Fig. 2. The essential feature of this plot is that rotational drag coefficient approaches $1.48\eta_m L^2$ for rods smaller than ℓ_0 and $0.5\eta_f L^3$ for rods longer than this natural length. (Both coefficients determined to 1%.) Thus, we find purely algebraic behavior in both limits.

Finally, to study the internal mode dynamics of a semiflexible inclusion, we consider the small transverse fluctuations of an infinitely thin, almost rodlike filament oriented along the x axis parametrized by $(x, r(x, t))$. With no slip boundary conditions on the inclusion, we have a dynamical equation for $r(x)$ to linear order,

$$\partial_t r(x, t) = \int dx' \chi(x - x', 0) \cdot (0, -\kappa \partial_x^4 r) + \theta(x, t), \quad (7)$$

where the thermal fluctuations $\theta(x, t)$ are chosen to satisfy the fluctuation-dissipation theorem. Expanding in modes of wave number q , we obtain a relaxation spectrum of transverse correlations given by

$$\langle \tilde{r}(q, t) \tilde{r}(q, 0) \rangle = \frac{2k_B T}{\kappa q^4} \exp[-t/\tau(q)], \quad (8)$$

where $\tau^{-1}(q) = [(2\kappa q^4)/\eta_m] \int_q^\infty \frac{dx}{2\pi} \{q^2/[x^2(x^2 - q^2)^{1/2}(x + \ell_0^{-1})]\}$. We have obtained a closed form expression for $\tau(q)$ that is plotted in Fig. 3. It is simple in the two limits of $q\ell_0 \ll 1$ and $q\ell_0 \gg 1$, where $\tau^{-1}(q \ll \ell_0^{-1}) \simeq (\kappa q^4)/(\pi\eta_f)$ and $\tau^{-1}(q \gg \ell_0^{-1}) \simeq (\kappa q^3)/(4\eta_m)$, respectively. At short scales, we find the dimensionally

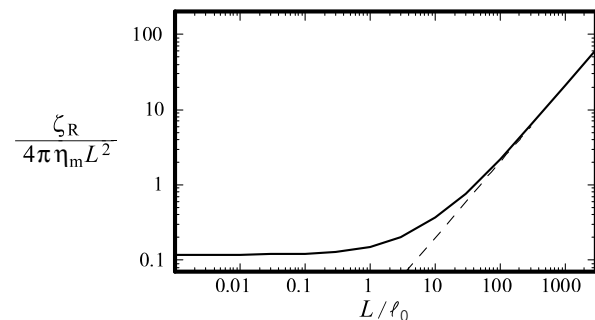


FIG. 2. The rotational drag coefficient of a rod of infinite aspect ratio plotted versus the length of the rod. The linear dependence (see text) is shown by the dashed line.

038102-3

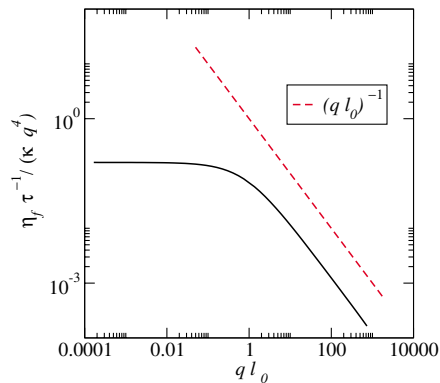


FIG. 3 (color online). The decay rate vs wave vector of transverse fluctuations of a semiflexible rod. The decay rate scaled by q^4 is wave vector independent for small q . Hydrodynamic interactions along the rod reduce the decay rate in a manner analogous to [17] for larger q .

reduced analogue of the hydrodynamic relaxation spectrum of fluid membranes ($D = 2$ dimensional manifold embedded in $D + 1$ dimensions) [17] (we consider $D = 1$). Here, though, the long-range hydrodynamic coupling crosses over to a purely *local* friction on the longest length scales [18,19].

We have calculated the translational and rotational hydrodynamic drag on a rod moving at low Reynolds number in a viscous film coupled to viscous subphase (and/or) superphase. When the dimensions of the rod are small ($\ll \ell_0$), the dissipation is governed primarily by the film, and the drag is insensitive to orientation and aspect ratio, and only weakly (logarithmically) dependent on size [6]. We find, surprisingly, that in the limit of a long rod ($\gg \ell_0$), the drag for motion perpendicular to the rod axis exhibits purely local drag per unit length. Thus, in contrast with motion in 3D fluids, there are no long-range hydrodynamic effects for long rods (for perpendicular motion), even though the dissipation occurs entirely in the fluid. A similar observation applies to rotational motion, and for the relaxation spectrum of the long wavelength modes of a semiflexible fluctuating filament, e.g., filamentous proteins in a viscous film. This is because, although the dissipation is governed primarily by the fluid, the film (along with its assumed incompressibility and no-slip conditions) imposes a very different boundary condition on the flow from what we would have in a bulk fluid alone. This added condition not only *increases* the drag for perpendicular motion relative to that without the film present, but results in purely local, or free-draining drag dynamics. In contrast, since the new boundary conditions *are* consistent with the standard flow field for parallel motion, we find quantitative agreement with the parallel mobility in a bulk fluid when the film's viscosity becomes irrelevant (small ℓ_0). Finally, we note that the methods developed here constitute a highly

adaptable framework to compute the mobility of arbitrary extended, irregularly shaped objects embedded in a viscous membrane or interface.

We thank D. K. Lubensky for generous discussions of his related work [19]. The work is supported in part by the National Science Foundation under Grants No. DMR98-70785 and No. PHY99-07949.

-
- [1] R. A. Stein, E. J. Hustedt, J. V. Staros, and A. H. Beth, *Biochemistry* **41**, 1957 (2002).
 - [2] P. J. R. Spooner, R. H. E. Friesen, J. Knol, B. Poolman, and A. Watts, *Biophys. J.* **79**, 756 (2000).
 - [3] K. Simons and E. Ikonen, *Nature (London)* **387**, 569 (1997).
 - [4] A. Pralle, P. Keller, E. L. Florin, K. Simons, and J. K. H. Horber, *J. Cell Biol.* **148**, 997 (2000).
 - [5] B. D. Hughes, B. A. Pailthorpe, and L. R. White, *J. Fluid Mech.* **110**, 349 (1981).
 - [6] P. G. Saffman and M. Delbrück, *Proc. Natl. Acad. Sci. U.S.A.* **72**, 3111 (1975). See also H. A. Stone, *J. Fluid Mech.* **409**, 165 (2000).
 - [7] H. A. Stone and H. M. McConnell, *Proc. R. Soc. London, Ser. A* **448**, 97 (1995).
 - [8] D. K. Lubensky and R. E. Goldstein, *Phys. Fluids* **8**, 843 (1996).
 - [9] H. A. Stone and A. Ajdari, *J. Fluid Mech.* **369**, 151 (1998).
 - [10] E. Helfer, S. Harlepp, L. Bourdieu, J. Robert, F. C. MacKintosh, and D. Chatenay, *Phys. Rev. Lett.* **85**, 457 (2000); E. Helfer, S. Harlepp, L. Bourdieu, J. Robert, F. C. MacKintosh, and D. Chatenay, *Phys. Rev. E* **63**, 021904 (2001).
 - [11] A. J. Levine and F. C. MacKintosh, *Phys. Rev. E* **66**, 061606 (2002).
 - [12] A. J. Levine, T. B. Liverpool, and F. C. MacKintosh, *Phys. Rev. E* **69**, 021503 (2004).
 - [13] C. F. Brooks, G. G. Fuller, C. W. Frank, and C. R. Robertson, *Langmuir* **15**, 2450 (1999); J. Q. Ding, H. E. Warriner, J. A. Zasadzinski, and D. K. Schwartz *Langmuir* **18**, 2800 (2002).
 - [14] T. M. Fischer, *J. Fluid Mech.* **498**, 123 (2004). Here, the author calculates the drag on a rod in a Langmuir film with subphase of finite depth. The technique developed is similar to ours, and a number of the same results have been obtained independently.
 - [15] Here, the *velocity* response function is $\chi = -i\omega\alpha$, where ω is the angular frequency and the *displacement* response function α is calculated in [11].
 - [16] S. F. Edwards, *The Theory of Polymer Dynamics* (Clarendon, Oxford, 1986).
 - [17] F. Brochard and J. F. Lennon, *J. Phys. (France)* **36**, 1035 (1975).
 - [18] That the drag coefficient per unit length of a fluctuating line becomes independent of wavelength in the long wavelength limit was noted in Ref. [8], and for circular domains in [7].
 - [19] D. K. Lubensky (unpublished).